analytical chemistry

Technical Note

pubs.acs.org/ac

Magnetic Detection of Mercuric Ion Using Giant Magnetoresistance-Based Biosensing System

Wei Wang,[†] Yi Wang,[†] Liang Tu,[†] Todd Klein,[†] Yinglong Feng,[†] Qin Li,[‡] and Jian-Ping Wang*[,†]

[†]Department of Electrical and Computer Engineering, University of Minnesota, Minneapolis, Minnesota 55455, United States

[‡]State Key Laboratory of Pollution Control and Resource Reuse, School of the Environment, Nanjing University, Nanjing 210046, China

Supporting Information

ABSTRACT: We have demonstrated a novel sensing strategy employing a giant magnetoresistance (GMR) biosensor and DNA chemistry for the detection of mercuric ion (Hg^{2+}). This assay takes advantages of high sensitivity and real-time signal readout of GMR biosensor and high selectivity of thymine−thymine (T−T) pair for Hg^{2+}. The assay has a detection limit of 10 nM in both buffer and natural water, which is the maximum mercury level in drinking water regulated by U.S. Environmental Protection Agency (EPA). The magnitude of the dynamic range for Hg^{2+} detection is up to three orders (10 nM to 10 μM). Herein, GMR sensing technology is first introduced into a pollutant monitoring area. It can be foreseen that the GMR biosensor could become a robust contender in the areas of environmental monitoring and food safety testing.

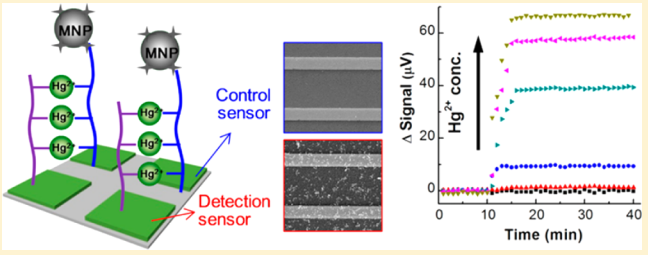

Contamination with mercury has been an important environmental and health concern throughout the world for decades. Mercuric ion (Hg^{2+}) is stable and soluble in aquatic systems, and high exposures may result in acrodynia (Pink disease) and damage to the nervous system and kidneys.[1] Furthermore, mercuric ion can be methylated and transform to methyl mercury by microbial biomethylation.[2] Methyl mercury can accumulate in bodies through the food chain, and it is known to cause brain damage and other chronic diseases, even paralysis and death.[3] Therefore, it is highly desirable to develop sensitive methods for the detection of Hg^{2+} in environmental monitoring. Traditional methods to detect mercury include atomic absorption spectrometry, cold vapor atomic fluorescence spectrometry, and inductively coupled plasma mass spectrometry, etc.[4] However, those tests are high cost, unportable, and rely heavily on central laboratories. Biosensor as a powerful and fast tool for molecular diagnostics is emerging recently. To date, several methods have been developed for the detection of mercuric ion using the electrochemical sensor,[5] triboelectric sensor,[6] surface plasmon resonance,[7] quartz crystal microbalance,[8] and quantum dots,[9] etc. Besides these techniques, one notable and fast-developing approach is using colloidal gold nanoparticles, which have been widely used in biomedical areas.[10] Gold nanoparticles are advantageous for Hg^{2+} detection in high sensitivity and selectivity, and feasible for in-field analysis while combining with small molecules,[11] proteins,[12] and DNA.[13]

A giant magnetoresistance (GMR) sensor has been widely and successfully used in the hard drive head since the late 1990s.[14] Its further application in biomolecular diagnostics has also emerged and been developed recently.[15] This GMR biosensing technology has the merits of low cost, high sensitivity, and real-time signal readout. The fabrication and integration of GMR biosensor are compatible with the current Very-Large-Scale Integration and System on Chip technologies, so it has great potential for eventually realizing point-of-care and portability with low cost. Furthermore, one of the fundamental advantages of the GMR biosensor is that the magnetic background of biological and environmental fluids is usually negligible. In contrast to colorimetric methods that require the use of light, there is no worry of magnetic signal interference by a sample matrix. However, to date, the application of GMR biosensor is mainly focused on proteins and nucleic acid assays.[16] It appears that GMR biosensor has not been used in environmental monitoring. It could be visualized that this GMR technology should have great application prospects in the environmental area by virtue of its powerful diagnostic capability. Driven by the need, we demonstrate in this article to detect mercuric ion (Hg^{2+}) using GMR biosensor technology. The final output signal for GMR biosensing is originated from a stray magnetic field, which is introduced by bound superparamgnetic magnetic nanoparticles (MNPs) on the GMR sensor surface. The bound MNPs are magnetized as the magnetic dipoles by an applied alternating magnetic field. Those magnetic dipoles generate the magnetic field that is sensed by the GMR sensor. A higher number of bound MNPs usually leads to a higher detection signal. Therefore, it is critical to build a detection model on the GMR

Received: December 11, 2013
Accepted: March 24, 2014
Published: March 24, 2014

   dx.doi.org/10.1021/ac404015j | *Anal. Chem.* 2014, 86, 3712−3716

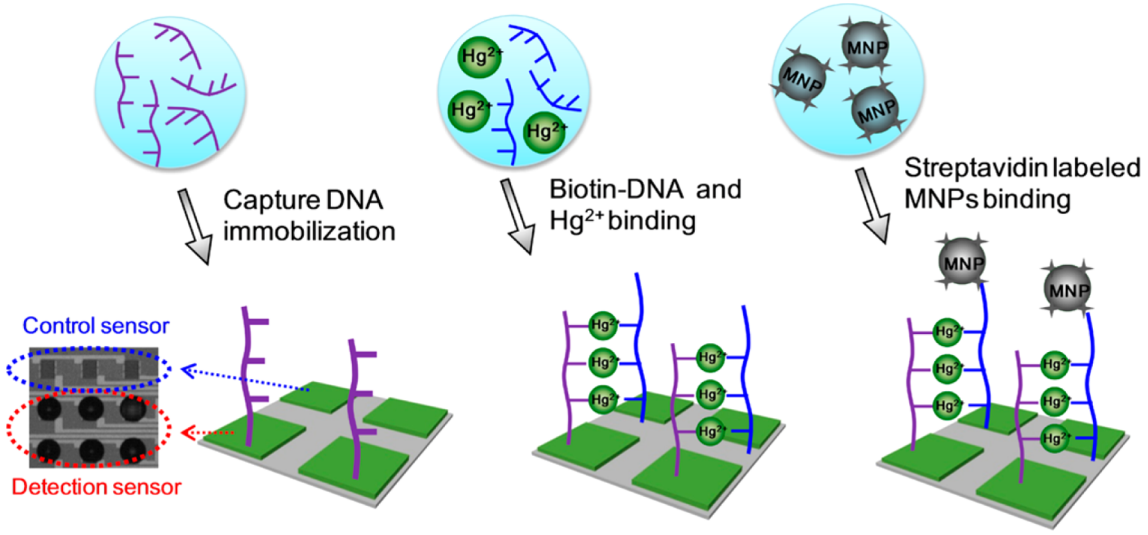

Figure 1. Schematic illustration of Hg^{2+} detection using the GMR biosensor.

sensor surface that the number of bound MNPs would be dependent on the amount of mercuric ions.

It was revealed that Hg^{2+} ions can specifically bind in between two DNA thymine bases and lead to the formation of a thymine−Hg^{2+}−thymine (T−Hg^{2+}−T) pair.[17] The Hg^{2+}-mediated T−T base pair was found to be at least as stable as normal Watson−Crick base pairs. Herein, this T−Hg^{2+}−T complex chemistry and complementary DNA with deliberately designed T−T mismatches are introduced and combined with a GMR biosensing system for sensitive and selective Hg^{2+} detection. The detection process is briefly illustrated in Figure 1. This detection architecture is similar to the sandwich DNA hybridization assay,[16] where the target DNA is replaced by the Hg^{2+}.

After capture, DNA oligmers are immobilized on the GMR sensor surface, biotin-labeled DNA (biotin-DNA) with T−T mismatches to capture DNA and Hg^{2+} are added. In the absence of Hg^{2+}, biotin-DNA would rarely be hybridized to immobilized capture DNA because of their mismatched base pairs. In contrast, the biotin-DNA can be bound and hybridized to the GMR sensor surface with the presence of Hg^{2+} due to the T−Hg^{2+}−T complex and Watson−Crick base pairing. The amount of bound biotin-DNA is expected to increase as the amount of added mercuric ions goes up, and finally lead to an increased number of MNPs after streptavidin-labeled MNPs are bound to the GMR sensor surface via the biotin−streptavidin interaction.

EXPERIMENTAL SECTION

GMR Chip Fabrication and Surface Functionalization. GMR spin valve films were deposited at the University of Minnesota with a Shamrock Magnetron Sputter System onto Si/SiO_2 (1000 Å) substrate. The multilayer films were top-down composed of Ta (50 Å)/NiFe (20 Å)/CoFe (10 Å)/Cu (33 Å)/CoFe (25 Å)/IrMn (80 Å)/Ta (25 Å). A GMR chip with 64 sensors (8 × 8 array) was fabricated with a photolithography technique (Figure S-2 of the Support Information).[18] Protective bilayers of 25 nm Al_2O_3 and 20 nm SiO_2 were finally coated on chip surface by ALD (atomic layer deposition) and PECVD (plasma-enhanced chemical vapor deposition), respectively. The bilayer was used to prevent leakage current, and surface SiO_2 was convenient for further surface functionalization.

The GMR chip surface was functionalized by 3-amino-propyltriethoxy silane (APTES) and glutaraldehyde (Glu). The process is briefly represented as follows. After thoroughly washing with acetone, methanol, and isopropanol, the chip was dried with nitrogen gas. The chip was dipped in 0.5% APTES solution (in toluene) for 15 min, and then it was washed with acetone and deionized (DI) water. The APTES modified chip was placed in a 5.0% Glu solution (in PBS buffer, 1×, pH 7.4) and incubated for 5 h, followed by being washed with DI water dried with nitrogen gas. After APTES-Glu modification, aldehyde groups were attached onto the sensor surface, so biomolecules containing amino groups, such as proteins and amine-labeled DNA can be immobilized on a GMR sensor surface.

Immobilization of Capture DNA and Hg^{2+} Binding. The capture DNA oligomer (5′/ACTAACTACTGTATC-CTGCA/3AmMC6T/3′) with amino modification at the 3′ end was purchased from Integrated DNA Technologies, Inc. It (20 nmol/mL in PBS buffer, 1×, pH 7.4) was spotted on individual GMR sensors, and part of the sensors in the same chip were retained and used as control sensors (Figure S-5 of the Supporting Information). The printed GMR chip was incubated for 24 h at room temperature under a relative humidity of ∼90%. After being rigorously rinsed with 0.2% SDS (sodium dodecyl sulfate) solution three times to remove unbound capture DNA, the chip was further washed with ultrapure water. For inactivating surplus aldehyde groups and reducing nonspecific binding, 20 μL of $NaBH_4$ solution [dissolving 1.0 mg $NaBH_4$ in 400 μL PBS (1 ×) and 100 μL ethanol] was added on the chip surface and incubated for approximately 5 min. After three washes with ultrapure water, the chip was immersed in hot water for several minutes to denature any annealed DNA. Then it was rinsed thoroughly with ultrapure water and dried with nitrogen gas. A bottomless reaction well made of polymethyl methacrylate (PMMA) was attached onto the chip surface. The reaction well can help to load a maximal liquid volume of 100 μL on the sensor array area. A mixture solution was made of 50 nmol/mL biotinylated DNA oligomer (5′/TGCTGGTTTCTGTTGTTTGT/Bio-tinBB-/3′, purchased from TriLink Biotechnologies), 0.01%

dx.doi.org/10.1021/ac404015j | Anal. Chem. 2014, 86, 3712−3716

tween 20, 10 mM HEPES buffer (pH = 7.5), 100 mM $NaClO_4$, and Hg^{2+} with desired concentrations (0, 10, and 100 nM and 1 and 10 μM). The Hg^{2+} solution was prepared from a concentrated stock solution (1 mM determined by cold vapor atomic fluorescence spectrometry). The mixture solution (100 μL) was loaded into the reaction well and incubated at 40 °C for 2 h. After that, the chip was washed with 0.2% SDS at room temperature for 5 min and rinsed with ultrapure water three times and then dried with nitrogen gas. The chip would be tightly sealed and kept in the refrigerator (4 °C) before its signal measurement.

Electronics and Measurement. Thirty microliters PBS solution was pipetted into the reaction well on the GMR chip that was connected to a GMR biosensing detection system (Figure S-1 of the Support Information). An alternating current at 1000 Hz and an alternating in-plane field of 30 Oe at 50 Hz were applied to each sensor. The amplitude of the mixing tone (1050 Hz) is measured as a primary output signal by a Fast Fourier Transform of the time-domain voltage signal from a data acquisition card (DAQ, NI USB-6289). A Wheatstone bridge setup shared by all 64 sensors is employed to eliminate the background analog signal, thus the small meaningful signal can be amplified and detected. Each measure takes about one second, so each sensor can get one data about every minute. After running for 10 min, 30 μL of MNP solution (roughly 3.14 pmol/mL) was added, and the detection signal generated by MNPs binding to sensor surface could be real-time recorded. The MNPs with a size of 50 nm were purchased from Miltenyi Biotech Inc. (catalog no. 130-048-102), and one MNP is composed of several 10 nm iron oxide cores embedded in the dextran matrix. The surface of MNPs is functionalized with streptavidin. These MNPs are dispersed and colloidally stable, so they do not aggregate and settle on the sensor surface.

RESULTS AND DISCUSSION

The fabrication process of the spin-valve type GMR biochip is described and shown in Figure S-2 of the Support Information. Its shape was visualized and confirmed under the optical microscope (Figure S-3 of the Support Information). The designed and fabricated GMR biochip in this work contains 64 GMR sensors, where each can work independently, and one 4 in. silicon wafer with a GMR multilayer stack can produce 21 full GMR biochips. Their fabrication cost could be dramatically reduced as a mass production process with a larger wafer (e.g., 12 in.) employed.

Concentrations of capture DNA and biotin-DNA oligmers are optimized for the Hg^{2+} assay (Figures S-6 and S-7 of the Support Information). We also examine a biochemical binding part of the experiment via a simple microarray-based fluorescence assay, and as expected, the fluorescence signal gets stronger as the Hg^{2+} concentration increases (Figure S-8 of the Support Information). The microarray images indicate that the background signal is very low. It proves that our experimental protocol for the biochemical binding part works well. As compared to the fluorescence assay, the GMR biosensor does not need central laboratory instruments and potentially realize in-field analysis. Most importantly, it is immune to background interference from environmental water samples. The real-time signals were detected and recorded using a benchtop GMR biosensing system (Figure S-1 of the Supporting Information). At present, the system is able to monitor up to 64 sensors in real-time, with a recording rate of 64 data points about every minute. Hence, one data can be recorded for each sensor in one minute. The typical real-time binding curves (signal vs time) for Hg^{2+} assays were shown in Figure 2a, and MNPs were added at 10 min. No obvious

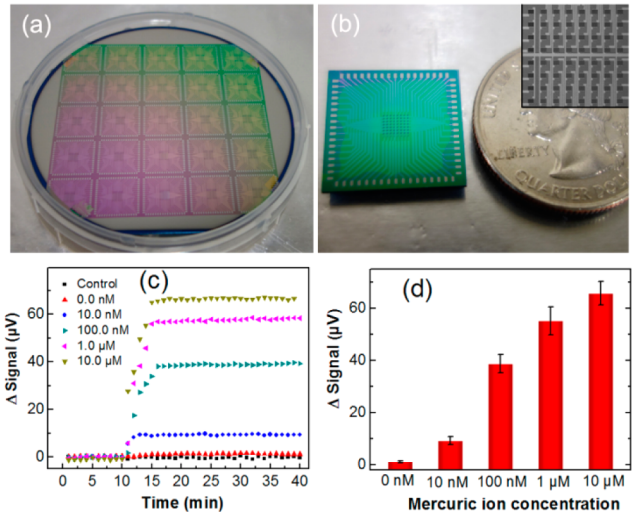

Figure 2. (a) One 4 in. silicon wafer can produce 21 full GMR chips and 4 fragmentary chips. (b) The size of GMR chip is comparative to the U.S. quarter coin. The 64 (8 × 8 array, inserted image) sensors were located in the central area of the chip, and each sensor was accordingly connected to peripheral contact pads on the periphery of the chip via contact lines. (c) Real-time binding curve data and (d) average signals [with standard deviation (SD)] for mercuric ions (Hg^{2+}) in buffer. Typically, the signal gains at time t = 30 min is used as the final signal of each sensor. Mean (SD) value of the signals from active sensors on the same chip are reported to compare different Hg^{2+} assay runs.

change is observed for the control signal (blank sensor), implying that few MNPs were bound to the control sensor surface. It is further verified by SEM analysis (Figure 3). The control signal is of great importance to GMR biosensing. It not only tells whether the testing is stable and repeatable but also indicates the influence of nonspecific binding. In absence of Hg^{2+} ([Hg^{2+}] = 0 nM), the signal is almost neglectable compared to the control signal line. The other signals for various Hg^{2+} concentrations show a rise beginning at t = 10

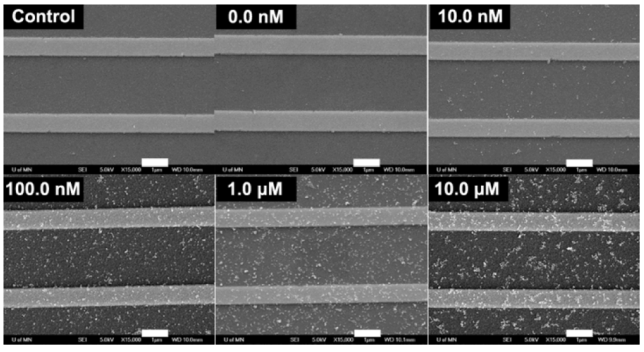

Figure 3. SEM images of MNPs bound on the GMR sensor surface after mercuric ions (Hg^{2+}) detection. All the scale bars are 1 μm. After the signal measurement was finished, the GMR chip was taken out and washed with water to remove any unbound MNPs immediately and then dried with nitrogen gas. The chip was coated with 5 nm Au film and further investigated by field emission scanning electron microscopy (FESEM, JEOL 6500).

dx.doi.org/10.1021/ac404015j | Anal. Chem. 2014, 86, 3712−3716

min. In this assay, the signal rising actually reflects a real-time MNP binding to the GMR sensor surface, on which biotin-DNA and Hg^{2+} have already been bound. The signal level for 10 nM Hg^{2+} saturates within 3 min, and reaching equilibrium for Hg^{2+} with a higher concentration takes about 5 min. More biotin-DNA are bound to the sensor surface as the Hg^{2+} concentration increases. It therefore takes a longer time to equilibrate for MNP binding. Furthermore, the binding time increases up to about 15 min as the saturated signal reaches 150−160 μV (Figure S-9 of the Support Information). The average signals for various Hg^{2+} concentrations are shown in Figure 2b. The LOD (limit of detection) of this assay is 10 nM (2 μg L^{-1}), which is the maximum contaminant level for mercury in drinkable water regulated by U.S. Environmental Protection Agency (EPA) in accordance with the authority of the Safe Drinking Water Act. The magnitude of dynamic range for Hg^{2+} detection using GMR sensing technology reaches up to 3 orders (10 nM to 10 μM). The average signal for 10 nM Hg^{2+} is about 9 μV, and it goes up with an increase in Hg^{2+} concentration. Hg^{2+} detection based on various methods is summarized in Table S-1 of the Support Information. It shows that the proposed GMR biosensor possesses quite a wide dynamic range and relative low detection limit for the detection of Hg^{2+} with respect to previous reports. The GMR signal responses were further confirmed by SEM analysis of the GMR sensor surface. As shown in Figure 3, the number of bound MNPs on the sensor surface obviously increases while increasing the Hg^{2+} concentration in the assay. GMR sensor of the 0 nM Hg^{2+} sample shows very few bound MNPs, while the bound number for the 10 μM Hg^{2+} sample is up to about 52/μm^2. The dependence of the GMR sensor signal on the number of bound MNPs is also analyzed (Figure S-11 of the Support Information). The result indicates that they have a good linear relationship (R^2 = 0.99).

In addition to the sensitivity, this GMR biosensing system also demands a high selectivity toward the Hg^{2+} ions. Previous studies have demonstrated that the T−T mismatch is very selective in binding to Hg^{2+} in different DNA-based Hg^{2+} testing systems, and a wide variety of metal ions do not show obvious interference with these methods.[5,13] To investigate the selectivity of the GMR sensing technique for the detection of Hg^{2+} ions, five common metal ions at a concentration of 1 μM were tested (Figure 4). It can be seen that all signal responses of the five metal ions are less than 10% of that of the mercuric ion. They are even weaker than the signal of Hg^{2+} at LOD concentration (10 nM). Thus, this GMR bioassay is also highly selective to Hg^{2+} detection. For the purposes of determining the capability of the GMR bioassay to detect Hg^{2+} in aqueous natural media, Hg^{2+} was spiked in water from Lake Minnetonka in Minnesota. The original concentration of total mercury in the lake water was determined to be below 12.5 pM (2.5 ng L^{-1}) by cold vapor atomic fluorescence spectrometry, which is far below the LOD of the assay. As detailed in Figure 5, the GMR bioassay is able to reliably test Hg^{2+} concentration up to 10 μM, and it also has a LOD of 10 nM for Hg^{2+} in natural water samples. As a new testing method for Hg^{2+}, there are multiple feasible strategies to further improve the sensitivity and dynamic range of this prototype GMR biosensing system in the future. First, the DNA sequences with designed T−T mismatches could be further optimized to bind Hg^{2+} more efficiently. Second, there is still a strong possibility of improving the magnetic performance of the GMR sensor by considering its shape, composition, and fabrication technology. Finally, MNPs have a significant impact on the GMR sensor signal according to our previous study,[15e,16c] thus choosing MNPs with superior quality (e.g., high-moment magnetic nanoparticles) would greatly improve the sensitivity.

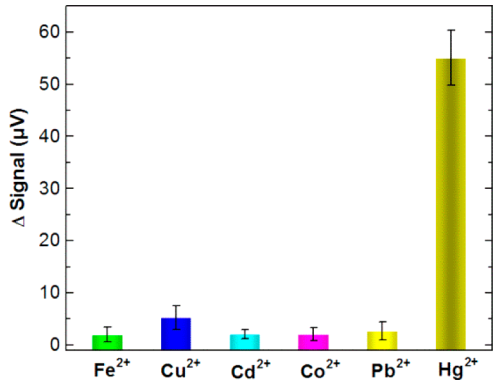

Figure 4. Average signals for various metal ions ([M^{2+}] = 1.0 μM). They are tested in a similar way as that of Hg^{2+} detection. Data was shown as mean ± SD.

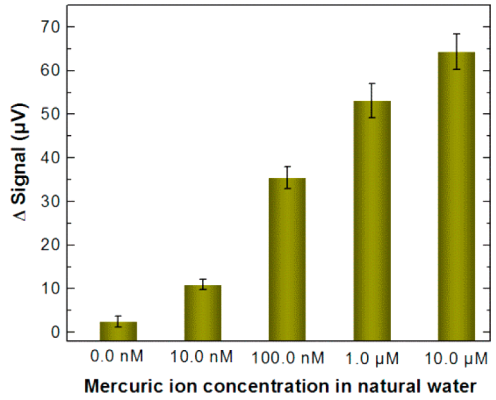

Figure 5. Average signals for various Hg^{2+} concentrations in natural water. Data was shown as mean ± SD.

CONCLUSION

In this work, a highly sensitive, selective, and real-time Hg^{2+} detection method using a GMR biosensing scheme combined with T−Hg^{2+}−T coordination chemistry was developed. A LOD of 10 nM in both buffer and natural water, which is the maximum mercury level in drinking water defined by the U.S. EPA, was achieved. Three orders of detection dynamic range (10 nM to 10 μM) in the GMR Hg^{2+} bioassay were obtained. On the basis of the features of GMR biosensing technology, this GMR Hg^{2+} bioassay is pointing toward a convenient and rapid field test. Furthermore, as a versatile and strong contender in molecular diagnostics, GMR bioassay not only can be applied in Hg^{2+} detection but also has great potential for the application of other pollutants monitoring in environment and food samples.

ASSOCIATED CONTENT

Supporting Information

Additional information as noted in text. This material is available free of charge via the Internet at http://pubs.acs.org.

dx.doi.org/10.1021/ac404015j | Anal. Chem. 2014, 86, 3712−3716

AUTHOR INFORMATION

Corresponding Author

*E-mail: jpwang@umn.edu.

Author Contributions

The manuscript was written through contributions of all authors. All authors have given approval to the final version of the manuscript.

Notes

The authors declare no competing financial interest.

ACKNOWLEDGMENTS

This work was partially supported by the Office for Technology Commercialization (OTC) and the resident fellows grant of the Institute on the Environment (IonE) at the University of Minnesota. Parts of this work were carried out in the Characterization Facility, University of Minnesota, which receives partial support from the National Science Foundation through the MRSEC program. We also thank Professor Ed Nater for the analysis of mercury.

REFERENCES

(1) Langford, N. J.; Ferner, R. E. *J. Hum. Hypertens.* **1999**, *13*, 651−656.

(2) Morel, F. M. M.; Kraepiel, A. M. L.; Amyot, M. *Annu. Rev. Ecol. Syst.* **1998**, *29*, 543−566.

(3) Grandjean, P.; Satoh, H.; Murata, K.; Eto, K. *Environ. Health Perspect.* **2010**, *118*, 1137−1145.

(4) (a) Ebdon, L.; Foulkes, M. E.; Le Roux, S.; Munoz-Olivas, R. *Analyst* **2002**, *127*, 1108−1114. (b) Li, Y. F.; Chen, C. Y.; Li, B.; Sun, J.; Wang, J. X.; Gao, Y. X.; Zhao, Y. L.; Chai, Z. F. *J. Anal. At. Spectrom.* **2006**, *21*, 94−96. (c) Butler, O. T.; Cook, J. M.; Harrington, C. F.; Hill, S. J.; Rieuwerts, J.; Miles, D. L. *J. Anal. At. Spectrom.* **2007**, *22*, 187−221.

(5) Wen, D.; Deng, L.; Guo, S.; Dong, S. *Anal. Chem.* **2011**, *83*, 3968−3972.

(6) Lin, Z. H.; Zhu, G.; Zhou, Y. S.; Yang, Y.; Bai, P.; Chen, J.; Wang, Z. L. *Angew. Chem., Int. Ed.* **2013**, *52*, 5065−5069.

(7) Abdi, M. M.; Abdullah, L. C.; Sadrolhosseini, A. R.; Yunus, W. M. M.; Moksin, M. M.; Tahir, P. M. *PLoS ONE* **2011**, *6*, e24578.

(8) Dong, Z. M.; Zhao, G. C. *Sensors* **2012**, *12*, 7080−7094.

(9) (a) Ke, J.; Li, X.; Shi, Y.; Zhao, Q.; Jiang, X. *Nanoscale* **2012**, *4*, 4996−5001. (b) Freeman, R.; Liu, X.; Willner, I. *J. Am. Chem. Soc.* **2011**, *133*, 11597−11604.

(10) (a) Rosi, N. L.; Giljohann, D. A.; Thaxton, C. S.; Lytton-Jean, A. K.; Han, M. S.; Mirkin, C. A. *Science* **2006**, *312*, 1027−1030. (b) Kim, D.; Jeong, Y. Y.; Jon, S. *ACS Nano* **2010**, *4*, 3689−3696.

(11) Vasimalai, N.; Abraham John, S. *Analyst* **2012**, *137*, 3349−3354.

(12) Guo, Y.; Wang, Z.; Qu, W.; Shao, H.; Jiang, X. *Biosens. Bioelectron.* **2011**, *26*, 4064−4069.

(13) (a) Lee, J. S.; Han, M. S.; Mirkin, C. A. *Angew. Chem., Int. Ed.* **2007**, *46*, 4093−4096. (b) Xue, X.; Wang, F.; Liu, X. *J. Am. Chem. Soc.* **2008**, *130*, 3244−3245. (c) Xia, F.; Zuo, X.; Yang, R.; Xiao, Y.; Kang, D.; Vallee-Belisle, A.; Gong, X.; Yuen, J. D.; Hsu, B. B. Y.; Heeger, A. J.; Plaxco, K. W. *Proc. Natl. Acad. Sci. U.S.A.* **2010**, *107*, 10837−10841.

(14) Tsang, C. H.; Fontana, R. E.; Lin, T.; Heim, D. E.; Gurney, B. A.; Williams, M. L. *IBM J. Res. Dev.* **1998**, *42*, 103−116.

(15) (a) Baselt, D. R.; Lee, G. U.; Natesan, M.; Metzger, S. W.; Sheehan, P. E.; Colton, R. J. *Biosens. Bioelectron.* **1998**, *13*, 731−739. (b) Schotter, J.; Kamp, P. B.; Becker, A.; Puhler, A.; Reiss, G.; Bruckl, H. *Biosens. Bioelectron.* **2004**, *19*, 1149−1156. (c) Janssen, X. J. A.; van IJzendoorn, L. J.; Prins, M. W. J. *Biosens. Bioelectron.* **2008**, *23*, 833−838. (d) Osterfeld, S. J.; Yu, H.; Gaster, R. S.; Caramuta, S.; Xu, L.; Han, S. J.; Hall, D. A.; Wilson, R. J.; Sun, S.; White, R. L.; Davis, R. W.; Pourmand, N.; Wang, S. X. *Proc. Natl. Acad. Sci. U.S.A.* **2008**, *52*, 20637−20640. (e) Srinivasan, B.; Li, Y.; Jing, Y.; Xu, Y.; Yao, X.; Xing, C.; Wang, J. P. *Angew. Chem., Int. Ed.* **2009**, *48*, 2764−2767.

(16) (a) Mulvaney, S. P.; Cole, C. L.; Kniller, M. D.; Malito, M.; Tamanaha, C. R.; Rife, J. C.; Stanton, M. W.; Whitman, L. J. *Biosens. Bioelectron.* **2007**, *23*, 191−200. (b) Martins, V. C.; Cardoso, F. A.; Germano, J.; Cardoso, S.; Sousa, L.; Piedade, M.; Freitas, P. P.; Fonseca, L. P. *Biosens. Bioelectron.* **2009**, *24*, 2690−2695. (c) Li, Y.; Srinivasan, B.; Jing, Y.; Yao, X.; Hugger, M. A.; Wang, J. P.; Xing, C. *J. Am. Chem. Soc.* **2010**, *132*, 4388−4392. (d) Zhi, X.; Liu, Q.; Zhang, X.; Zhang, Y.; Feng, J.; Cui, D. *Lab Chip* **2012**, *12*, 741−745.

(17) Ono, A.; Togashi, H. *Angew. Chem., Int. Ed.* **2004**, *43*, 4300−4302.

(18) Wang, W.; Wang, Y.; Tu, L.; Klein, T.; Feng, Y.; Wang, J. P. *IEEE Trans. Magn.* **2013**, *49*, 296−299.

NOTE ADDED AFTER ASAP PUBLICATION

This paper was published ASAP on April 4, 2014. Typographical changes were made in the title and text and the revised version was reposted on April 15, 2014.